



Global Climatology of Low-Level-Jets: Occurrence, Characteristics, and Meteorological Drivers

E. W. Luiz¹  and S. Fiedler^{1,2} 

¹Institute for Geophysics and Meteorology, University of Cologne, Cologne, Germany, ²Now at GEOMAR Helmholtz Centre for Ocean Research Kiel, Faculty for Mathematics and Natural Sciences, Christian-Albrechts-University Kiel, Kiel, Germany

Key Points:

- First global comprehensive low-level jet (LLJ) climatology using ERA5
- Polar LLJs are the strongest and most frequent among the detected types
- Distinct past trends in regional LLJ frequency and intensity

Supporting Information:

Supporting Information may be found in the online version of this article.

Correspondence to:

E. W. Luiz,
eweidetu@uni-koeln.de

Citation:

Luiz, E. W., & Fiedler, S. (2024). Global climatology of low-level-jets: Occurrence, characteristics, and meteorological drivers. *Journal of Geophysical Research: Atmospheres*, 129, e2023JD040262. <https://doi.org/10.1029/2023JD040262>

Received 24 OCT 2023

Accepted 9 APR 2024

Author Contributions:

Conceptualization: E. W. Luiz, S. Fiedler
Data curation: E. W. Luiz
Formal analysis: E. W. Luiz
Funding acquisition: S. Fiedler
Investigation: E. W. Luiz
Methodology: E. W. Luiz
Project administration: S. Fiedler
Supervision: S. Fiedler
Validation: E. W. Luiz
Visualization: E. W. Luiz
Writing – original draft: E. W. Luiz
Writing – review & editing: E. W. Luiz, S. Fiedler

Abstract Low-level jets (LLJs), vertical profiles with a wind speed maxima in the lowest hundred meters of the troposphere, have multiple impacts in the Earth system, but a global present-day climatology based on contemporary data does not exist. We use the spatially and temporally complete data set from ERA5 reanalysis to compile a global climatology of LLJs for studying the formation mechanisms, characteristics, and trends during the period of 1992–2021. In the global mean, LLJs are detected 21% of the time with more cases over land (32%) than over the ocean (15%). We classified the LLJs into three categories: non-polar land (LLLJ), polar land (PLLJ), and coastal (CLLJ) LLJs. For LLLJ, the averaged frequency of occurrence is 20% and 75% of them are associated with a near-surface temperature inversion as a prerequisite for an inertial oscillation. PLLJs are also associated with a temperature inversion and occur even more frequently with 59% of the time. These are also the lowest and the strongest LLJs among the three categories. CLLJs are particularly frequent in some marine hotspots, situated along the west coast of continents, with neutral to unstable stratification close to the surfaces and a stably stratified layer aloft. We found distinct regional trends in both the frequency and intensity of LLJs over the past decades, which can have implications for the emission and transport of aerosols, and the transport of atmospheric moisture. Future studies could address changes in LLJs and the associated implications in more detail, based on the here released ERA5-based LLJ data.

Plain Language Summary In this study, we investigated low-level jets (LLJs), and strong winds in the lower atmosphere that have significant environmental and societal impacts. Using a comprehensive weather data set spanning from 1992 to 2021, we created a global map of LLJs, categorizing them into three regions: non-polar land (LLLJ), polar land (PLLJ), and coastal (CLLJ). LLJs associated with temperature inversions were very common over land, but PLLJs were much more frequent. PLLJs were also the strongest and lowest. Coastal LLJs were prevalent on west coastlines and exhibited changing vertical temperature characteristics. On average, LLJs occurred 21% of the time globally, with higher frequencies over land (32%) compared to the ocean (15%). Regional trends in LLJ frequency and intensity varied, with some areas experiencing more intense LLJs without changes in frequency while others presented an increase in both. The study emphasized the uncertainty surrounding the influence of LLJs on climate and weather extremes in a warming world, with future research aiming at exploring LLJ trends and their broader implications.

1. Introduction

Low-level jets (LLJ) are wind speed maxima in the lowest few hundred meters of the troposphere (Shapiro & Fedorovich, 2010; Ziemann et al., 2020). LLJs show a sharp decrease in wind speed above their core leading to the characteristic nose-like wind speed profile. They have diverse influences spanning from environmental to societal impacts, for example, transport of moisture and pollutants (Angevine et al., 2006; R. Chen & Tomassini, 2015), aviation safety (Blackadar, 1957; Wittich et al., 1986), formation of dust storms (Schepanski et al., 2009) and wind power production (Gutierrez et al., 2016; Lampert et al., 2016; E. W. Luiz & Fiedler, 2022). Furthermore, LLJs are perceived as a mechanism for (sub)tropical moisture transport (Gimeno et al., 2016). They are also linked to the spatio-temporal variability of precipitation in certain regions, influencing the availability of freshwater for consumption, agriculture, and ecosystems (Algarra et al., 2019). LLJs therefore play a role in the hydrological cycle (Pan et al., 2004), including the occurrence of droughts and floods (Algarra et al., 2019). Moreover, LLJs over coastal waters influence sea-surface temperatures by driving the upwelling of cold nutrient-rich waters with implications for the regional ecosystems and economic activities (Semedo et al., 2016).

© 2024 The Authors.

This is an open access article under the terms of the [Creative Commons Attribution-NonCommercial License](https://creativecommons.org/licenses/by/4.0/), which permits use, distribution and reproduction in any medium, provided the original work is properly cited and is not used for commercial purposes.

In the classical theoretical description of inertial oscillations, LLJs develop due to the decoupling of nocturnal winds from the surface friction by the formation of a near-surface temperature inversion (Blackadar, 1957; B. J. Van de Wiel et al., 2010). These conditions typically occur over land at night, particularly during cloud-free conditions that allow strong radiative cooling near the surface (Beyrich, 1994; Sisterson & Frenzen, 1978). The associated weaker friction due to reduced eddy viscosity enables acceleration of the airflow aloft (Fiedler et al., 2013; Ziemann et al., 2020), with the development of a pronounced super-geostrophic wind speed maximum in the course of the night (Shapiro & Fedorovich, 2010). Such undisturbed inertial oscillations are a widely known formation mechanism of LLJs and are often called Nocturnal LLJs (NLLJ). In reality, the development of NLLJs diverts from the ideal fully decoupled and undisturbed inertial oscillation that was theoretically described by Blackadar (1957), due to reduced but not eliminated frictional effects (B. J. Van de Wiel et al., 2010), the occurrence of intermittent turbulence at night (B. Van de Wiel et al., 2003) and non-stationary environmental conditions (E. W. Luiz & Fiedler, 2022). Moreover, LLJs with a co-occurring temperature inversion can also be driven by other mechanisms, for example, in the absence of nocturnal cooling. For example, LLJs can be formed when a near-surface temperature inversion is formed by warm air advection over relatively cool near-surface air. The associated tilt of the isobaric surfaces leads to a thermal wind that under certain conditions can manifest itself as a LLJ. LLJs have further been connected to synoptic and mesoscale dynamical systems (G. T.-J. Chen et al., 2006; Corrêa et al., 2021; Li & Du, 2021; E. Luiz & Fiedler, 2023).

LLJs are known to occur in different regions around the world that favor the development of different types. Common locations for LLJ occurrence are coastal upwelling regions (Lima et al., 2022), hot deserts (Fiedler et al., 2013; Heinold et al., 2013) and continental polar regions (Heinemann & Zentek, 2021; Tuononen et al., 2015). LLJs in hot desert areas are usually NLLJs, although a fraction of the LLJs are connected to convective cold pools (Heinold et al., 2013). LLJs in hot deserts have strong implications for forming dust storms (Fiedler et al., 2013; Z. Han et al., 2022). Likewise, LLJs happening in continental polar regions (PLLJs), or cold deserts, are generated by the stabilization of the atmospheric boundary layer via near-surface cooling or warm air advection (Heinemann & Zentek, 2021). Other mechanisms for LLJ formation over cold deserts were also identified. The topography, for example, can lead to the formation of barrier winds, katabatic flows, and tip jets, all of which may form wind profiles that can meet the LLJ criteria (Tuononen et al., 2015). In zones of high baroclinicity, such as synoptic or mesoscale fronts along an ice edge, the vertical shear of the geostrophic wind and surface friction can lead to the generation of baroclinic LLJs (Heinemann et al., 2021; Jakobson et al., 2013).

Coastal low-level jets (CLLJs) usually occur offshore of the west coast of different continents, for example, USA, Chile/Peru, Australia, and Africa (Lima et al., 2022), with seasonal differences that depend on the region. In general, the differential heating leads to the formation of a high-pressure system over the ocean and a thermal low over land. The associated pressure differences lead to strong winds. Since the warm air subsides in the high pressure above the Marine Atmospheric Boundary Layer and cooler, moist, and well-mixed air resides above the ocean surface, the development of a temperature inversion in some distance to the surface is favored (Beardsley et al., 1987). Reduced frictional effects in the inversion layer allow the formation of a CLLJ, which is not unlike the condition for an NLLJ, but occurs in this case also during the day and at higher levels, with a maximum usually in the lowest 1,000 m a.g.l. (Garreaud & Muñoz, 2005; Ranjha et al., 2013; Soares et al., 2014). CLLJs are also frequently detected in the Caribbean region (Amador Astúa, 1998), where they are also inversely connected to the frequency of tropical cyclones. There, the stronger summer winds (July–August) imply a stronger than normal vertical wind shear at low-levels, which are unfavorable conditions for tropical cyclone development (Amador et al., 2010).

Multiple studies for individual processes driving LLJs in different world regions exist, yet there is no global climatology accounting for more than single LLJ types with details on their relative occurrence frequencies, characteristics, and past trends based on contemporary data. In the present study, we take advantage of the spatially and temporally complete meteorological data with a sufficiently high spatial and temporal resolution as provided by the ERA5 reanalysis for 1992–2021 and an automated detection algorithm for LLJs to better understand LLJs from a global perspective. As we will see later, ERA5 is adequate for compiling a global LLJ climatology. Our focus is on (a) the global quantification of differently driven LLJs, (b) the characterization of governing physical processes of LLJs in occurrence hotspot regions distributed across the world, and (c) an assessment of past trends for LLJs with global warming. In so doing, we present a comprehensive global climatology of LLJs accounting for the different physical driving mechanisms for their development and release the newly compiled ERA5-based LLJ data.

2. Data and Methods

2.1. ERA5

ERA5 is the latest global reanalysis data set from the European Centre for Medium-range Weather Forecasts (ECMWF) (Hersbach et al., 2020). ERA5 combines a state-of-the-art weather model with historical measurements (satellites, weather stations, etc.) to obtain a spatially and temporally consistent data set covering the years since 1940. ERA5 provides global output for many different meteorological variables (Y. Han et al., 2021) on a grid with a horizontal resolution of about 30 km and 137 vertical levels. About 20 levels are within the first 1,000 m a.g.l. giving a suitable vertical resolution to study LLJs. The temporal resolution of the output is variable, with hourly intervals being the finest resolution. For this work, we used data for wind speed, humidity, temperature and pressure on the model levels with a three-hourly resolution for 1992–2021 to compile the LLJ climatology over 30 years.

2.2. LLJ Detection and Classification

The identification and analysis of the LLJs in ERA5 are based on an automated detection algorithm developed earlier for the ERA-Interim reanalysis of ECMWF (Fiedler et al., 2013). We follow the same approach, except that we here do the initial identification of LLJ based on the wind speed profiles alone. This choice allows the additional identification of LLJs that are not formed in the presence of a near-surface temperature inversion for a holistic analysis of different LLJ types. The criteria in the algorithm are set such that the algorithm detects LLJs with a characteristic nose-like wind profile as in Fiedler et al. (2013) and E. W. Luiz and Fiedler (2022). The LLJ core was identified as the wind speed maximum in the lowest 1,000 m a.g.l. that satisfies the following criteria. First, a low-level wind speed maximum is identified as an LLJ if the vertical shear in the wind speed is more negative than 0.005 s^{-1} in the 500 m deep layer above the LLJ core. Second, we require a difference in the wind speed between the same layers of at least 2 ms^{-1} . Both these criteria ensure a nose-like profile and exclude ambiguous cases. The detection algorithm was applied to every three-hourly wind profile in ERA5 for the 30-year time period of 1992–2021. The statistical analysis like the calculation of the frequency of occurrence of LLJs is based on the profiles, that is, we calculate the fraction of profiles with a LLJ relative to the total number of profiles. For the comparison to measurements from radiosondes with data availabilities of every 6–12 hr, we selected the ERA5 profiles corresponding to the same time as the radiosondes and calculated the total number of profiles with LLJs.

The analysis of the outputs included a separation of the LLJs into three different regions. LLJs in non-polar land areas, where NLLJs following the classical inertial oscillation theory at night are expected, were called land LLJ (LLLJ). LLJs in polar land regions, which we will see also often are NLLJs, were called Polar LLJ (PLLJ). LLJs in coastal waters within a distance of 20 grid points from a coast were called Coastal LLJ (CLLJ). The latter follows a different formation mechanism than NLLJ, as we show later. Figure 1 marks the locations, in which we assessed the dynamics of the different LLJ types at the mentioned regions. We selected places where LLJ profiles frequently occur and aimed for a global distribution that covers different regional climates. From each of those regions, the grid point with the highest frequency of occurrence was selected to better understand the dynamics of LLJs through performing composite analyses. The selected regions are the following.

- A location in Antarctica and in Greenland were selected for studying PLLJs.
- For CLLJ, six locations over the ocean were picked. The Benguela current and the coasts of West USA, Chile/Peru, West Africa, West Australia, and Oman.
- LLLJs were analyzed in the hot desert climates of the Saharan desert in Chad in North Africa and the Taklamakan desert in China, a region with a semi-arid climate in Brazil and a temperate climate in Germany.

For the dynamical assessment of the LLJs, we used two different metrics for the atmospheric stability and the momentum flux, namely the vertical gradient in the virtual potential temperature ($\Delta\theta_v$) and the Richardson Number (Ri). A stably stratified air layer is characterized by an increase of θ_v with height. We here require $\Delta\theta_v > 0.001 \text{ Km}^{-1}$ for stable conditions to inform us about the co-occurrence of inversions with LLJs. Moreover, Ri provides information on the influence of the tendency of shear-induced vertical mixing which can be strong during LLJs. Large Ri values imply that the effect of the stable stratification is stronger than the effect of shear-driven turbulent mixing. The critical threshold for the transition between stable and unstable conditions is about 0.25, that is, turbulence occurs when Ri is smaller than this threshold (Peng et al., 2022). The characteristics of the

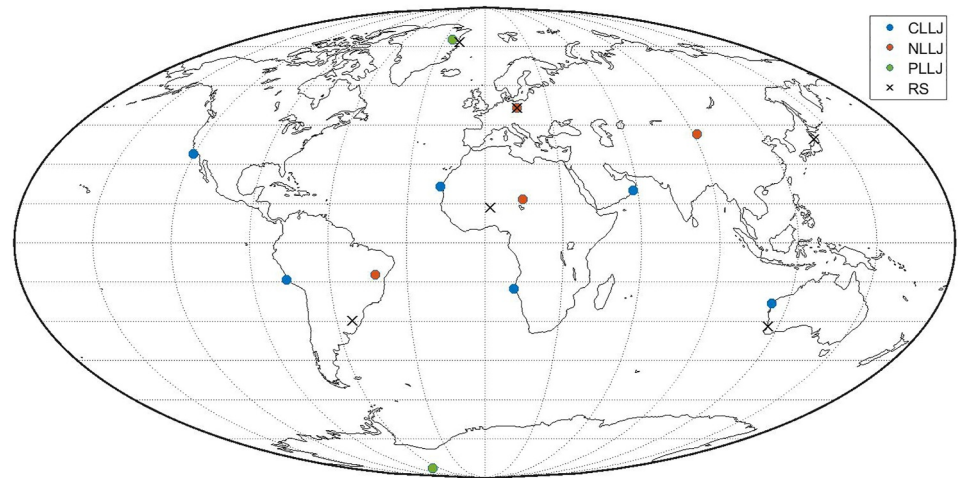


Figure 1. Location of the grid points selected for the analysis of LLJ types and the radiosonde (RS) sites for the evaluation of LLJs in ERA5.

LLJs are calculated as composite means, that is, the means are calculated for the LLJ cores of all profiles with an LLJ. To visually highlight seasonal differences in the LLJ characteristics, we compute their difference for the summer hemispheres against the annual means.

2.3. Validation of Approach

We validated to what extent observed LLJs are reproduced by ERA5, applying the automated detection algorithm for LLJs to co-located profiles from ERA5 and radiosondes. To that end, we selected stations with quality-controlled radiosondes (RSs), obtained from the department of Atmospheric Science of the University of Wyoming. The chosen stations encompass different climates around the world and are situated in Perth (Australia), Lindenberg (Germany), Santa Maria (Brazil), Niamey (Niger), Danmakshavn (Greenland), and Akita (Japan). Figure 1 shows the locations of the analyzed sites. Although some of the RSs have been assimilated, it is useful to make this comparison. ERA5 for instance also assimilates data from satellite measurements and surface meteorological stations, assigns different weights to the different data sets for generating the analysis, performs an interpolation of the observation in time and space to match the model grid, and also depends on the forecast model state at the time of assimilation which is jointly influencing the analysis. Hence, we expect differences in the LLJs in RSs and ERA5 which we indeed see, but the general temporal variability of LLJs follows very similar patterns in across the different sites assessed here.

Specifically, the month-to-month variability in detected LLJs from the RSs is well reproduced by ERA5. Figure 2 shows the monthly co-variability of the number of LLJ profiles in ERA5 and the RSs during 1 year at the sites. We calculated the Probability of Detection (POD) as the probability of ERA5 detecting a LLJ profile when a LLJ was identified by the radiosonde. The False Alarm Rate (FAR) is the probability of ERA5 identifying an LLJ when there was no detection by the radiosonde. From the selected sites, the POD ranged from 0.47 in Lindenberg (Germany) to 0.73 in Perth (Australia). FAR ranged from 0.32 in Akita (Japan) to 0.6 in Niamey (Niger). Testing other sites than the ones included here led to similar results (not shown). It suggests that the month-to-month variability in the LLJ frequency of occurrence is reasonably well represented by ERA5. Also, the characterization of the LLJs by ERA5 is sufficiently good for our purposes. The average wind speed at the LLJ core was for instance very similar in ERA5 and the RSs ($\sim 11 \text{ ms}^{-1}$) with the LLJ core heights being underestimated by ERA5, with an average of 417 m in ERA5 against 537 m in the RSs of the analyzed sites. Note that the global average and averages over other sites can deviate from these numbers. For example, the ERA5 average LLJ core in Lindenberg (Germany) was slightly higher in ERA5, while in Santa Maria (Brazil) and Niamey (Niger), they were much lower.

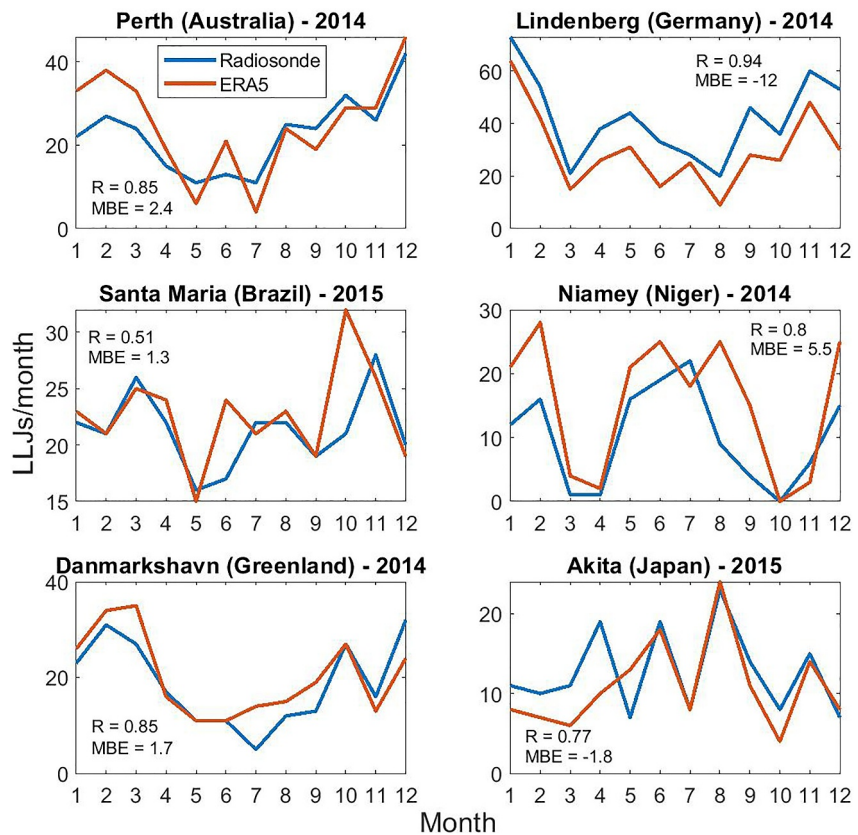


Figure 2. Validation of LLJ profiles occurrence frequency in ERA5. Shown are the monthly mean number of LLJs detected with radiosondes (blue) and in ERA5 (red) at different sites. The comparison was done for the years 2014 or 2015, as stated in the title of the figures, due to the availability of radiosonde data. The selection of the sites (see Figure 1) covers different climatic conditions.

3. Results

3.1. Global LLJ Occurrence

The global climatology of the frequency of occurrence of LLJs highlights several regional hotspots, including the continental polar regions and the offshore regions off the west coast of continents. Moreover, hot desert regions frequently witness LLJs, for example, the Sahara and the Taklamakan deserts. Figures 3a–3c show the global frequency of LLJs averaged for all months, for winter and summer. A more detailed view of the frequency of occurrence at different regions is shown in Figures S5–S12 of the Supporting Information S1. Some regions show a pronounced seasonal variability in the LLJ occurrence frequency. Take for instance the Australian West Coast and Oman's East Coast, which have a maximum LLJ occurrence in just one of the two seasons (Figures 3b and 3c). Other regions have relatively similar LLJ occurrence throughout the year with slight differences in the exact location of the regional maximum, for example, a small North-South difference in the maximum at the West African Coast. Also the land regions near the poles, namely Greenland and Antarctica, frequently see LLJs which are slightly more often occurring during polar night.

Figures 3d–3i show the frequency of occurrence of LLJs in the presence of a temperature inversion layer. Here, we compute the atmospheric stability based on the vertical gradient in the virtual potential temperature from the surface until the LLJ core (Figures 3d–3f) and in the lowest 100 m a.g.l. (Figures 3g–3i). LLJs in the absence of an inversion layer are typically less frequent. Coastal LLJs typically have no near-surface temperature inversion (e.g., in the lowest 100 m a.g.l.), but present it accounting for all layers below the LLJ core, as indicated by the higher frequency of occurrence of LLJs for these conditions. Over regions offshore of coasts, we typically see a well-mixed marine boundary layer at the lowest levels underneath the LLJ core with an inversion above it. Most LLJs without an inversion in the lowest levels happen over the ocean at up-welling regions west of the continents.

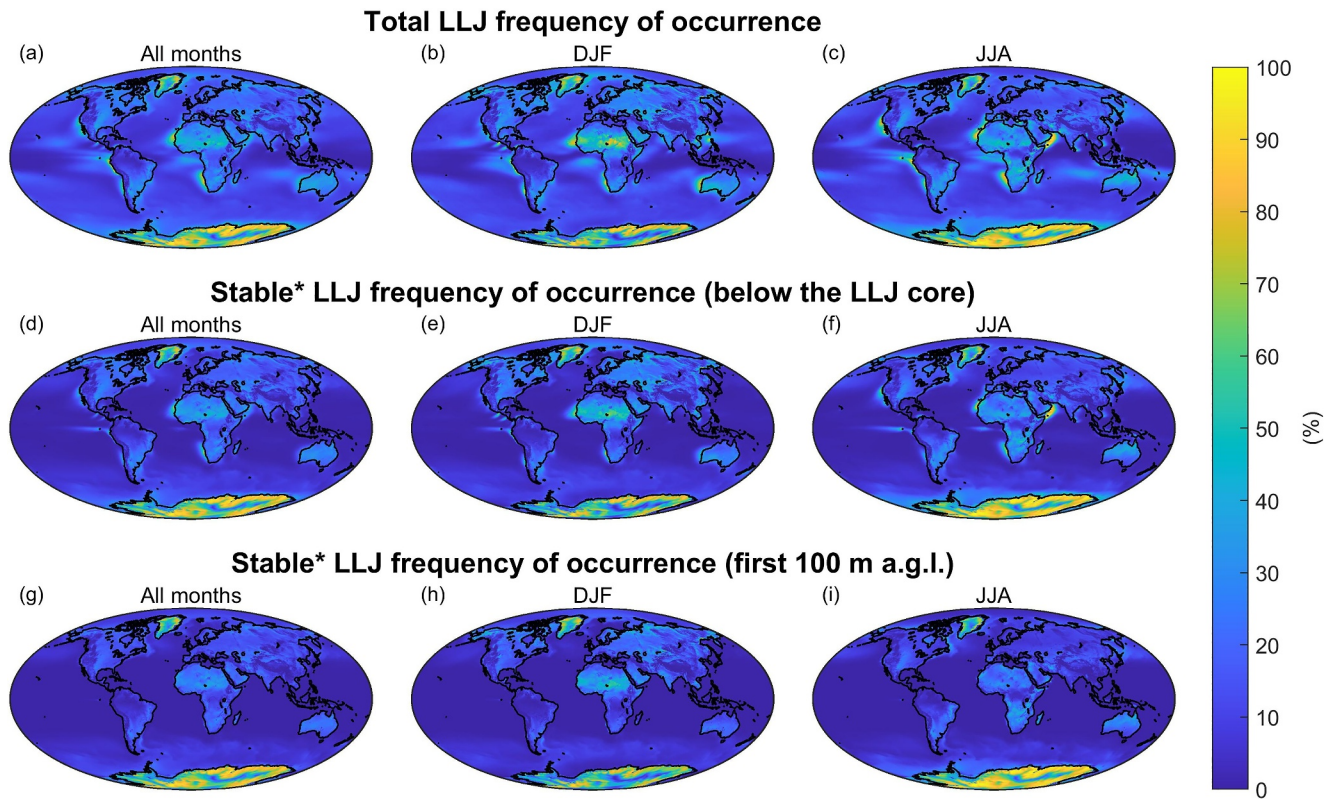


Figure 3. Spatial patterns of the occurrence frequency of LLJs in percent of all profiles. Shown are (a–c) the total frequency of occurrence of LLJs, (d–f) the frequency of occurrence of LLJs during stable conditions from the surface until the LLJ core, and (g–i) the same as (d–f) but for the lowest 100 m a.g.l. The left column shows the mean over all months, the middle for December, January, and February (DJF), and the right column for June, July, and August (JJA). *Stable LLJs were considered when $\Delta\theta_v > 0.001 \text{ Km}^{-1}$, that is, when we found the presence of a temperature inversion. The results are based on ERA5 for 1992–2021. Regional maps where we zoom in for more spatial details are shown in Figures S4–S12 of the Supporting Information S1.

On land, most of the LLJs happen with the presence of a near-surface temperature inversion, with formation mechanisms connected to inertial oscillations. During NLLJ, we still have a lower amount of weaker LLJs when the temperature inversion is broken by surface warming, which may account for the LLJs without the inversion presence. A detailed analysis of the vertical structure of the atmosphere for the different LLJ types and regions will be done in the next chapters.

The global mean in the frequency of occurrence of LLJs is 21%. It is important to mention that this is an average over all grid points and the regions closest to the poles have a higher weight. The mean frequencies for LLJs with a simultaneous appearance of an inversion measured by $\Delta\theta_v > 0.001 \text{ Km}^{-1}$ from surface until the LLJ core (in the lowest 100 m a.g.l.) occur in 15% (12%) of the profiles. The slight difference in the occurrence frequency of the LLJs with inversion layers at different altitudes can be explained by the neutral to unstable stratification close to ocean surfaces that become more stably stratified with increasing height. Specifically, the frequency of occurrence of LLJs averaged over oceans for all LLJ cases, with a stable stratification below the LLJ core and those with a surface temperature inversion in the lowest 100 m a.g.l is 15%, 8%, and 5%, respectively. On land, the differences associated with a temperature inversion are less apparent, with average frequencies of occurrence of LLJs of 28%–32%. On average, the frequency of occurrence of LLJs on land is higher than over the oceans, because many regions over the ocean have very small LLJ frequency of occurrence. This can be seen by the mask made for regions with a frequency of occurrence smaller than 15% from Figure 4.

3.2. Global LLJ Characteristics

Globally averaged, the mean wind speed of LLJs is about 12 ms^{-1} , with a difference at the order of 10% ($<1 \text{ ms}^{-1}$) when we compute the average over ocean and land regions separately. The mean height of the LLJ cores differs more between the ocean with 419 m against land with 325 m. The global average of the LLJ core

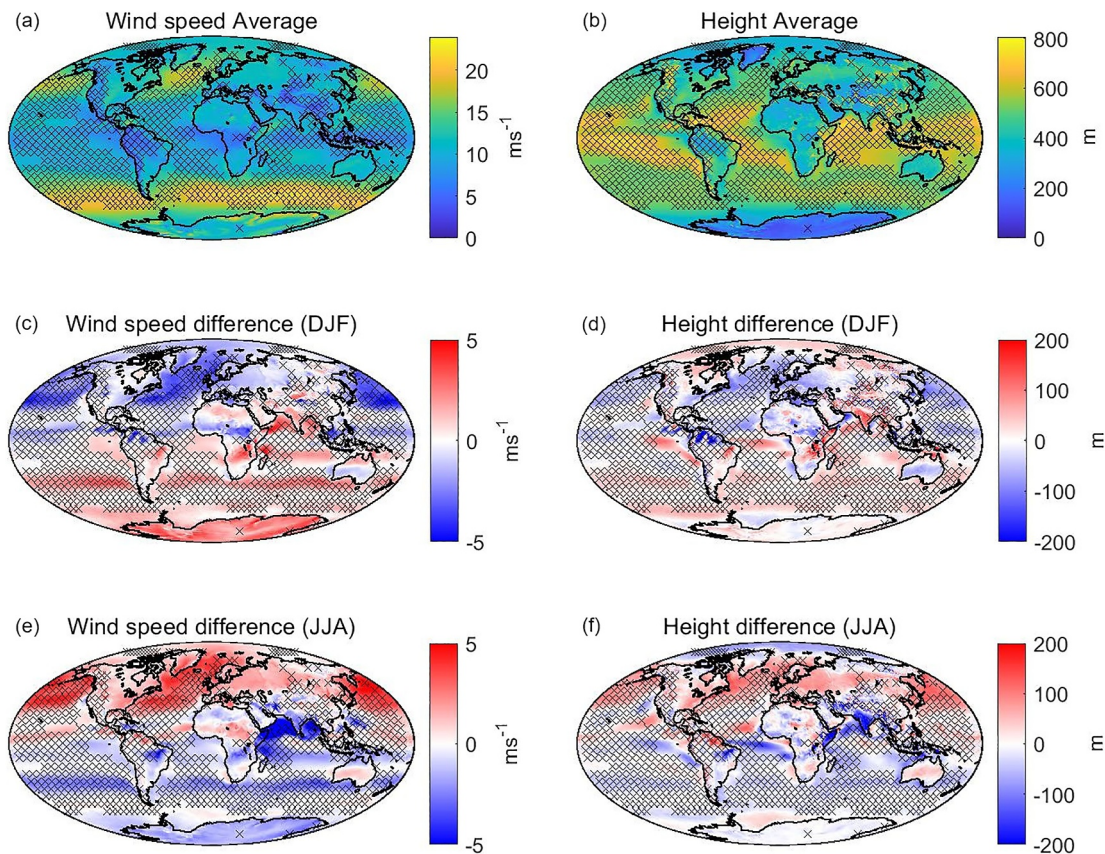


Figure 4. Spatial patterns of LLJ characteristics. Shown are the averages of the (a) wind speeds and (b) heights in the core of LLJs calculated as composite means over all detected LLJs, and (c–f) the differences in the characteristics in the mean for December, January, and February (DJF), and for June, July, and August (JJA) relative to the annual means shown in (a) and (b). The dashed areas mask regions where the LLJ frequency of occurrence was smaller than 15%. The results are based on ERA5 for 1992–2021.

height is 371 m. Accounting for the co-occurrence of a temperature inversion for LLJs has a marginal influence on the globally averaged wind speed and height of the LLJ cores. The average height of LLJs for regions with frequencies of occurrence higher than 15% and a co-occurring temperature inversion, measured by $\Delta\theta_v > 0.001 \text{ Km}^{-1}$ underneath the LLJ core, is for instance 387 m.

Figures 4a and 4b show the spatial patterns of wind speed and height of the LLJ cores averaged for 1992–2021 with a mask over the regions with the frequency of occurrence smaller than 15%. The value of 15% was chosen in this study as an objective criterion to analyze the regions with the main LLJ types defined here. The LLJ heights in both Antarctica and Greenland are less than 200 m a.g.l. which is lower compared to most other regions. The wind speed in the core of LLJs in these cold deserts is around 12 ms^{-1} which is stronger compared to most other land regions. Over ocean regions, stronger wind speeds in LLJ cores are seen in the extra-tropical storm tracks of both hemispheres, at around latitudes of 50° . Here the LLJ profiles can be connected with frontal systems associated with extra-tropical cyclones. We also see for instance a maximum in the LLJ core wind speed for the Caribbean LLJ (Figure 4a), consistent with Torres-Alavez et al. (2021). Interestingly, the height of LLJ cores increases over oceans from the poles toward the equator, consistent with the deeper boundary layer over warmer tropical waters relative to cooler sea-surface temperatures toward the poles.

Seasonal differences in the LLJ intensity show a remarkably consistent hemispheric asymmetry, with typically stronger (weaker) LLJs across most of the summer (winter) hemisphere compared to the annual mean (Figures 4c–4f). The asymmetry in the LLJ strength is most pronounced in the extra-tropics than in the tropics consistent with the stronger seasonal variation in near-surface temperatures. Typically higher summertime boundary layers over land in the extra-tropics also lead to regionally higher LLJ cores relative to the annual mean, for example, for many mid-latitude regions in the northern hemisphere and over Australia during the summer

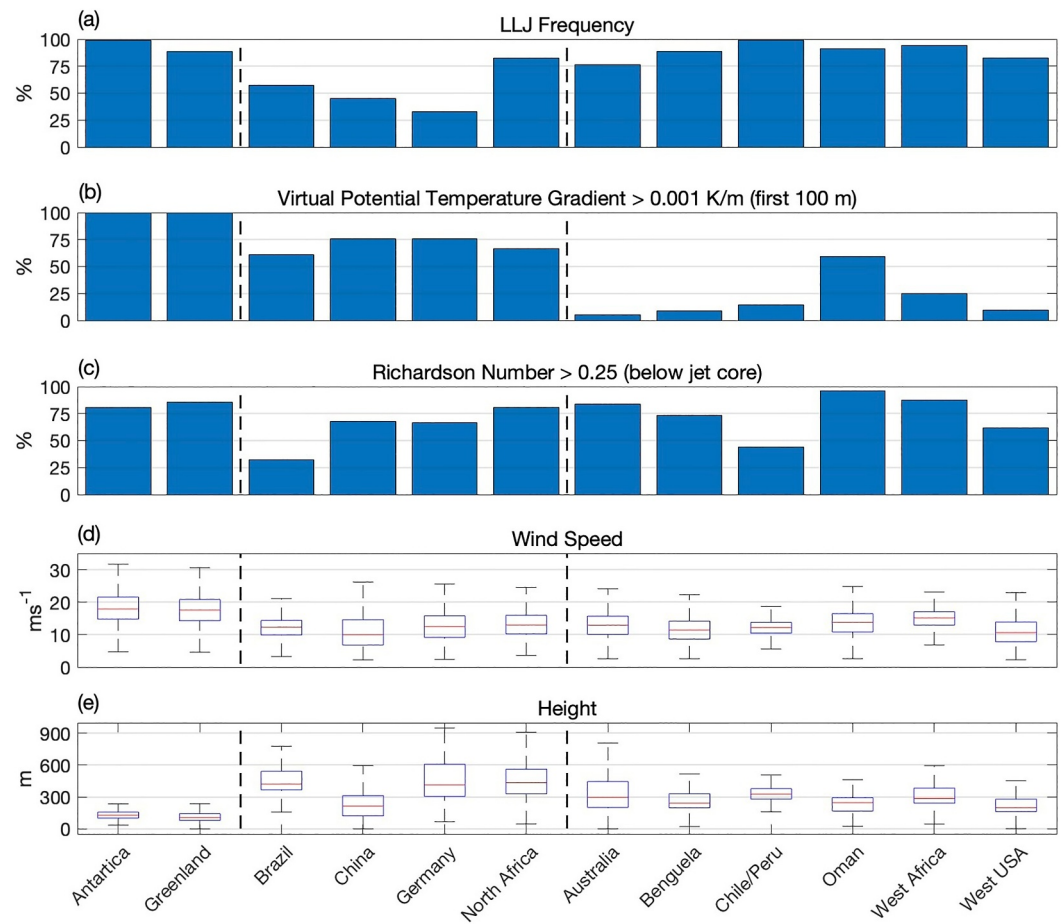


Figure 5. Statistics of different LLJ types at the selected locations. Shown are the (a) LLJ frequency of occurrence in % of all profiles, (b) percentage of LLJs with co-occurring virtual potential temperature gradient of $\Delta\theta_v > 0.001 \text{ Km}^{-1}$ in the lowest 100 m a.g.l., (c) percentage of LLJs with the Richardson Number > 0.25 below the LLJ core, (d) statistics of the wind speed and (e) height of the LLJ cores showing the means (red), quartiles (box), and the 25 and 75 percentiles (whiskers). The vertical dashed lines separate (left to right) PLLJs, LLLJs, and CLLJs. The locations are marked in Figure 1.

seasons. An interesting opposite behavior of the described seasonality of the regional LLJ characteristics in the extra-tropics is seen along the coast of Oman. Here, the wind speed and height of the LLJ cores are higher (lower) during the winter (summer) months compared to the annual mean, with a seasonally different driving mechanism: the Indian Monsoon (Ranjha et al., 2015).

3.3. LLJ Regions

We analyze LLJ dynamics in more detail for the three different regions inspired by existing classifications from the literature (see Section 2 for details), namely non-polar land low-level jets (LLLJs), coastal low-level jets (CLLJs) and polar low-level jets (PLLJs). Examples of averaged wind profiles for the year 2018 are found in Figure S1 of the Supporting Information S1 from all locations marked in Figure 1. PLLJs were the strongest and lowest LLJs amongst the locations assessed here. In Antarctica, LLJs can have core wind speeds exceeding 20 ms^{-1} at heights well below 200 m a.g.l.. The PLLJs are, therefore, much lower than LLJs formed by reduced dynamical friction in hot deserts. The LLLJs locations presented the highest cores compared to all LLJ locations assessed, for example, the Bodélé Depression in Chad, North Africa, has high NLLJ cores around 500 m a.g.l. in the mean for 2018.

We systematically assessed the regional LLJ differences by statistical analyses over the entire 30-year period with Figure 5, including atmospheric stability metrics, height, and speed of the LLJ cores as well as the frequency of occurrence of the LLJs. Again, we can see the lower heights and higher wind speeds of PLLJs, while the highest

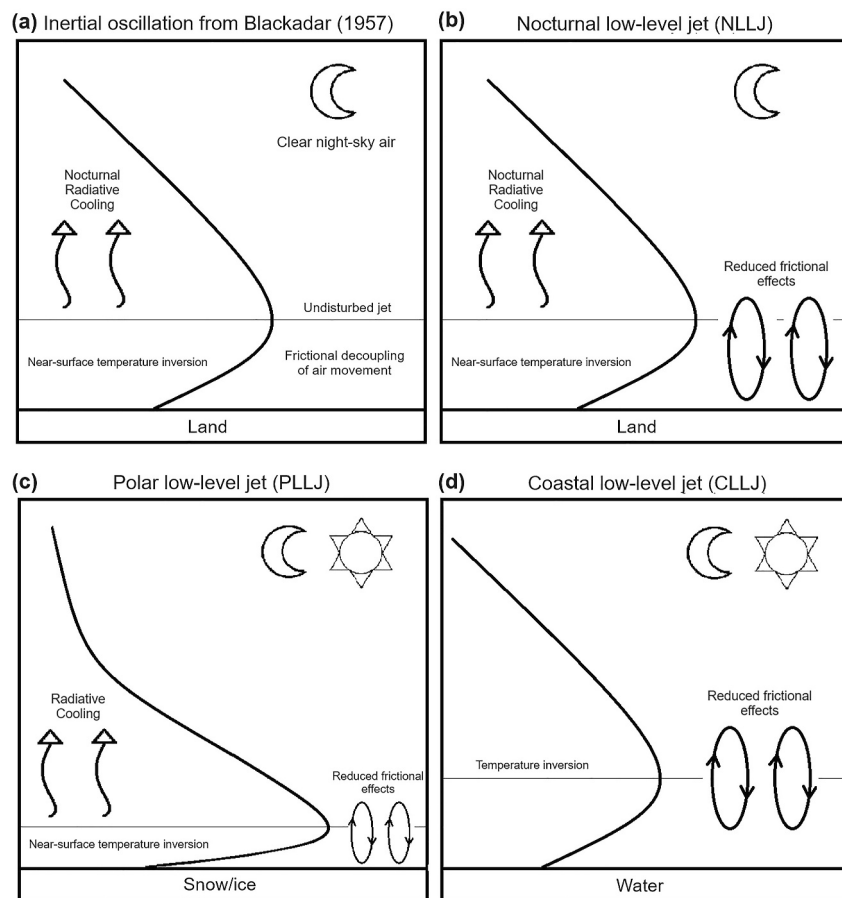


Figure 6. Schematic diagram of different LLJ types. Depicted are the conditions for the theory of an inertial oscillation (Blackadar, 1957) and the LLJ types analyzed in this study.

LLJs are found at the LLLJ locations. CLLJs and LLLJs have similar wind speed characteristics. Most LLLJs coincide with stable stratification directly below the LLJ core, which allows for the balance of shear-induced mixing of momentum by the LLJ. This can be seen by the high simultaneity of LLJs and Richardson Numbers larger than 0.25 from the surface until the LLJ core. The Brazilian site is an exception with less than 50% of the LLJs having Richardson numbers exceeding 0.25. It implies that the LLJs here are typically less stable compared to the other locations, which implies some downward mixing of momentum. This aspect is further assessed in the following.

3.3.1. Non-Polar Land Low-Level Jets (LLLJ)

LLLJ regions also have a high frequency of NLLJs, which are formed by a mechanism similar to an inertial oscillation and usually occur during the night, when radiative cooling allows the formation of a near-surface temperature inversion. These mechanisms are schematically depicted in Figures 6a and 6b following the idealized theory of an inertial oscillation from Blackadar (1957) and accounting for non-stationary effects that are common in reality. The average frequency of occurrence over LLLJ areas is about 20%, with 75% of them coinciding with a near-surface temperature inversion. From the picked LLLJ locations (Figure 5), more than 50% of the LLLJ profiles coincide with a near-surface temperature inversion, measured by a mean of $\Delta\theta_v > 0.001 \text{ Km}^{-1}$ over the lowest 100 m a.g.l.. Similarly, a stable stratification underneath most LLLJ locations allows a relatively stable development of LLJs, as measured by $\text{Ri} > 0.25$.

To better understand the development of NLLJs, Figures 7a and 7b show a case study for an NLLJ in North Africa with a wind speed profile that is closest to the mean NLLJ profile for 2018. We see the transition from a well-mixed daytime boundary layer to the evening formation of a near-surface inversion. It implies increasing

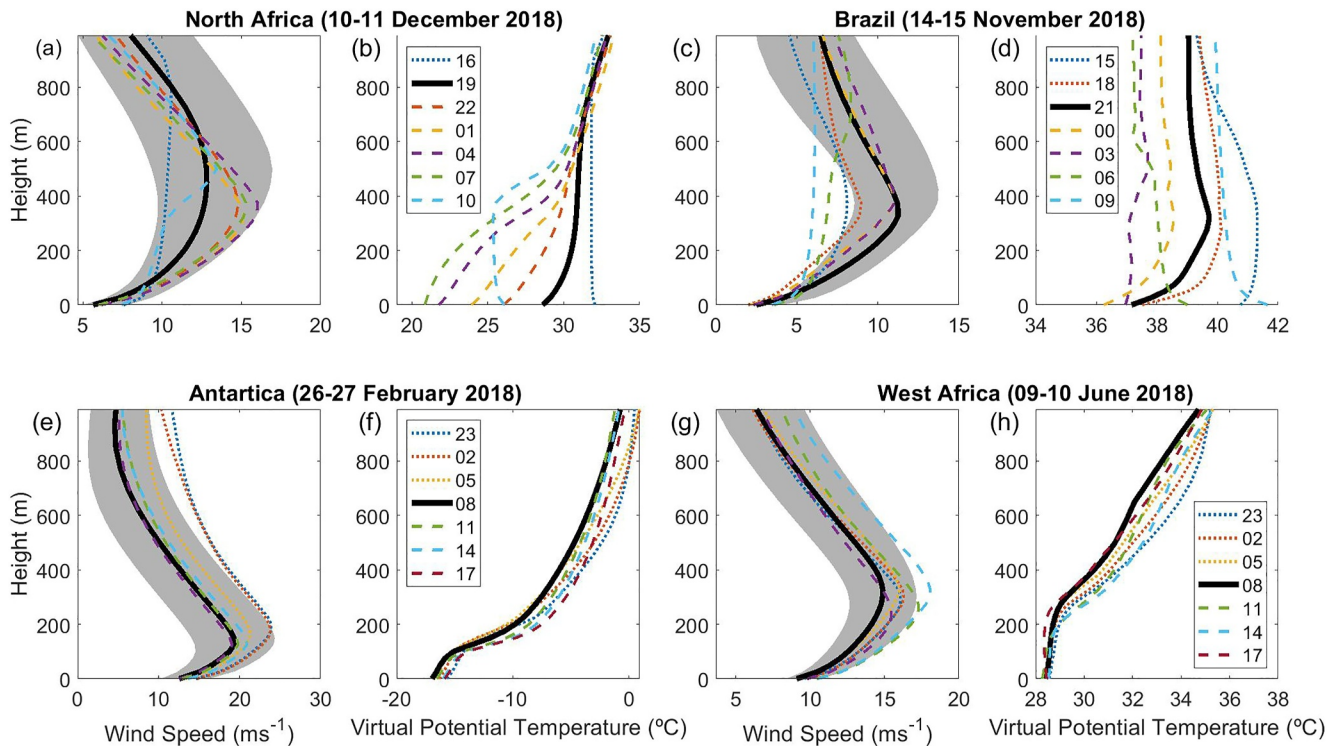


Figure 7. Case studies for the development of different LLJ types representative of their respective mean at the same location. Shown are the vertical profiles of (left) the wind speed and (right) the virtual potential temperature for the LLJ location and time stated in the title. The solid black lines are the wind profile of the selected LLJ that is most similar to the average for the LLJs at the same location in 2018. Shading marks the area of $\pm 1\sigma$, one standard deviation. Colored lines are the profiles for different hours before and after the selected LLJ to illustrate their development.

static stability after sunset (19 LST) initially seen as an increase in θ_v with height close to the surface. This development continues by further surface cooling, deepening of the inversion layer up to 600 m a.g.l. in the course of the night. Simultaneously an NLLJ develops with the characteristic nocturnal acceleration of the air motion several hundred meters above the surface with a maximum at 04 LST and a subsequent slight deceleration associated with the turning of the wind field driven by the Coriolis force. The mid-morning breakdown of the NLLJ is associated with morning heating leading to a well-mixed boundary layer at 10 LST. At that time, the momentum of the NLLJ has been transferred to the surface and the core now appears about 100 m higher than at night.

The development of NLLJs at the Brazilian location can behave differently causing the lowest number of stable LLJs (compare Figure 5). Figures 7c and 7d show the case study for an NLLJ in Brazil that is close to the 2018 mean. The wind speed profile of the NLLJ has characteristics similar to North Africa. However, in Brazil the inversion and hence the stability during the NLLJ was much weaker directly underneath the NLLJ and shallower until midnight compared to North Africa. The inversion decayed already during the night, specifically a well-mixed boundary layer is seen at 03 LST interrupting the nocturnal acceleration of the air motion. The momentum is subsequently transferred toward the surface causing the disappearance of the NLLJ already at 06 LST, much earlier than in North Africa.

In both case studies the wind speed in the core of the NLLJ is sub-geostrophic throughout the lifetime and there is no ideal change in the wind direction over time as one would expect from the theory of Blackadar (1957) (not shown). Deviations from the theory are to be expected since the assumption of stationarity is not fulfilled. Some cases, however, can show supergeostrophy. We see, for instance, for the NLLJ case study for Germany, a clear circular cyclonic change in the wind direction in the course of the night leading to a supergeostrophic wind speed in the NLLJ core, for example, at 23 LST and 01 LST (Figure S2 in Supporting Information S1). Supergeostrophy is expected from the theory but it is predicted to be a much smoother and gradual development, indicating that also in this case study non-stationary effects influenced the development of the NLLJ.

3.3.2. Polar Low-Level Jets (PLLJ)

PLLJs are common throughout the year and mostly co-occur with a temperature inversion (Figure 5), namely in 90% of the cases in Antarctica and Greenland. The average frequency of occurrence of PLLJ over Antarctica and Greenland is very high, about 59%; with some locations having values above 90%. This is broadly consistent with previous studies (e.g., Heinemann & Zentek, 2021; Tuononen et al., 2015). The development of PLLJs is similar to inertial oscillations that one expected due to near-surface inversion formed by little irradiance in polar nights causing low surface temperatures throughout the day for several months (Figure 6c). The very high frequency of LLJs coinciding with a near-surface temperature inversion (99%) at PLLJ regions suggests other different driving mechanisms than NLLJs, since they also happen during daytime. PLLJs can then be further favored by the cold surface, complex topography, and baroclinicity (Tuononen et al., 2015).

Figures 7e and 7f show a case study for Antarctica. It shows a snapshot of a long-lived PLLJ with a core at around 100 m with wind speeds of more than 20 ms^{-1} . It occurs during stably stratified conditions that show only little variation over time with a particularly strong inversion around the LLJ core. Similar conditions can also be seen in Greenland (not shown). The case studies at both locations also showed a circular change of the wind direction over time, with a clockwise (anticlockwise) turning in Greenland (Antarctica) due to the Coriolis force. The selected case shown here for Antarctica also reached supergeostrophic wind speeds in the LLJ core, but this is not always the case, as suggested by the subgeostrophic PLLJ in a case assessed over Greenland (not shown).

Most continental LLJs, thus PLLJs and NLLJs have wind directions depending on the regional weather patterns causing differently oriented geostrophic wind vectors (Figure S3 in Supporting Information S1). Interestingly, they have a clearly prevailing direction per location. North African NLLJs, for instance, primarily have north-easterly directions (Figure S4 in Supporting Information S1), consistent with earlier findings based on another reanalysis (Fiedler et al., 2013). The largest spread in LLJ directions is seen for the location in Germany, consistent with different weather patterns driving LLJs there (E. W. Luiz & Fiedler, 2022).

3.3.3. Coastal Low-Level Jets (CLLJ)

Most CLLJs form offshore off the west coast of continents. On average, the frequency of occurrence over the coast (19%) is a bit higher than the frequency of occurrence over all ocean (15%). Differently from LLLJ regions, we can see some hotspots with values close to 90% for the CLLJ regions. These LLJs develop under different conditions than NLLJs and PLLJs (Figure 6d). CLLJs are rarely associated with a near-surface temperature inversion. They occur most often during neutral to unstable atmospheric conditions in the mean over the lowest 100 m a.g.l.. The case study for West Africa shows that the boundary layer is rather neutral stratified close to the surface and becomes stably stratified around the CLLJ core (Figures 7g and 7h). Above the LLJ core, θ_v particularly strongly increased with height; indicative of a stable stratification. Amongst CLLJ locations, Oman has most frequently a near-surface inversion, but this is still about 50% of the cases; less frequent than for PLLJs and most LLLJs (Figure 5b).

Depending on their location, CLLJs might undergo a strong seasonal cycle. The Benguela CLLJ, for example, can occur throughout the year, with differences in its mean frequency and the location of the maximum. Such differences depend primarily on the zonal pressure gradient near the surface (Lima et al., 2019). Differently, the seasonal cycle of CLLJ in Australia is strong, with a maximum in the frequency of occurrence during austral summer. The Oman CLLJ is unique by its location, synoptic forcing and its link to South Asia Monsoon (Ranjha et al., 2015). Hence it behaves differently throughout the year, with a maximum frequency of occurrence during July and August. The wind directions of CLLJs are typically parallel to the coastlines and usually toward the equator (Figures S3 and S4 in Supporting Information S1), consistent with the prevailing wind direction in the trades. Again, Oman is the exception due to its different dynamical forcing. Other CLLJs are worth to mention, for example, the Caribbean LLJ, with the strongest regional increase in the frequency of occurrence during the past decades, and the Papagayos, south of Costa Rica, which are linked to low-level stable stratifications during winter, like seen during the advection of cold air (Luna-Niño & Cavazos, 2018).

3.4. Past Changes of LLJs

We assess to what extent LLJs might have changed during the past decades by computing linear trends (Figure 8a). The global averaged frequency of occurrence trend is $0.02\%/year$. There are regionally positive trends

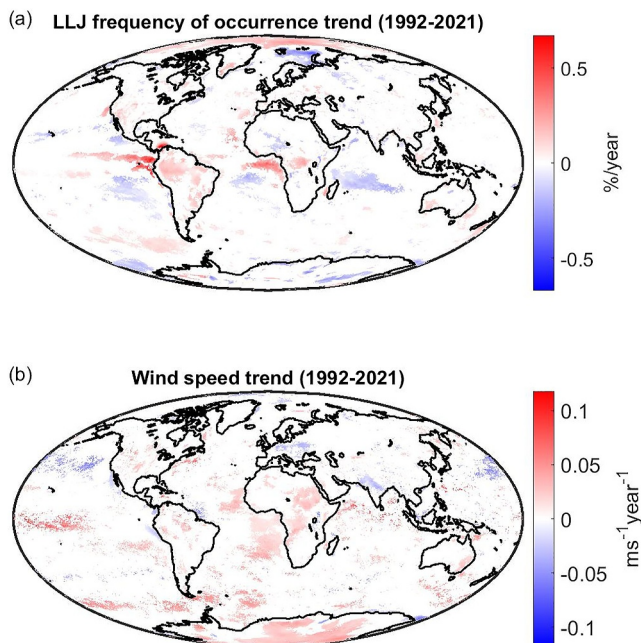


Figure 8. Past trends for LLJs for 1992–2021. Shown are the statistically significant linear trends in (a) the frequency of occurrence of LLJs and (b) the wind speed in the LLJ core. The results are based on ERA5 and for a 95% level of significance using the Mann Kendall test.

in the annually averaged frequency of occurrence of LLJs in the Arctic and eastern equatorial regions of the Atlantic and Pacific. The location with the largest positive trend is seen in the southern part of the Caribbean Sea, in the Caribbean LLJ region. The positive trends in the Arctic and also in southern Greenland and western USA were especially strong during boreal winter. Amongst the selected locations for case studies, Chile/Peru had also an increase in the LLJ frequency of occurrence over time that is statistically significant at the 95% level of significance. Negative trends in the frequency of occurrence of LLJs are seen in the southern Indian Ocean, and to the southwest of the regions with positive trends in the Atlantic and Pacific. There is also a strong negative trend in the Barents Sea, which is most pronounced during boreal winter. Also, Northeast of the Oman LLJ region, a strong negative trend was seen during boreal summer, but is not seen in the annual mean. Amongst the locations for case studies, only Chile/Peru presented a positive trend.

Trends in the LLJ core wind speed (Figure 8b) are typically negative (positive) North (South) of 20° North, with a global average of $0.02 \text{ ms}^{-1} \text{ year}^{-1}$. Most positive trends are seen over Antarctica, central and northeast Africa, and offshore of the western coasts of Africa. Negative trends were detected over central and eastern Europe, northern India, and the northern Pacific. Amongst the locations for case studies, Antarctica, Chile/Peru, North Africa, and West Africa had positive trends in the LLJ wind speed, whereas Germany had a negative trend.

4. Discussion

Some regions have seen higher frequency and intensity of LLJs over the past 30 years. Over the Amazon region, for example, the mean frequency of occurrence is relatively low, but our results indicate an increase in their frequency and intensity. These trends can imply changes in the precipitation in the Southern Amazonia and the La Plata River Basin. For instance, the amount of atmospheric moisture transported by the South American LLJ is comparable to the Amazon River (Arraut et al., 2012). This may increase the climate change impacts related to changes in land use (particularly deforestation) due to its influence on the water cycle (Zemp et al., 2014).

LLJs frequently form in desert areas such as Northern Africa (Fiedler et al., 2013). The NLLJs in Northern Africa play an important role in emitting mineral dust into the atmosphere (Heinold et al., 2013; Knippertz & Todd, 2012; Schepanski et al., 2009), which are known for several different impacts in the Earth system (Prospero et al., 2002; Washington et al., 2003). In some parts of North Africa, specifically in the Sahel, our results suggest a decreasing frequency of occurrence but little change elsewhere. The intensity of NLLJs, however, has increased over comparably larger regions in eastern parts of North Africa, including the Bodélé Depression in Chad which has been named as the dustiest place on Earth. These trends might have led to a change in regional dust storm frequency and intensity, for example, a tendency to more intense dust storms associated with NLLJs in the Bodélé Depression and beyond.

Changes in LLJs over the ocean can have implications for the transport of moisture, known to play a role in the hydrological cycle in several regions of the world, for example, for the Asian monsoon systems. In particular, the Gulf of Bengal and the Indian Ocean function as primary reservoirs of moisture for the India Monsoon LLJ, the Southeast Asia Monsoon LLJ, and the China Monsoon LLJ (Algarra et al., 2019). We found no significant changes in the frequency of occurrence of the India Monsoon LLJ. However, in offshore regions along the coast of Oman and Somalia, we can see an increase in the LLJ intensity, while Northern India experiences a negative trend in the mean LLJ wind speed. These changes may have repercussions on the moisture advection potentially affecting precipitation formation downwind during the Indian summer monsoon.

We can see large areas with positive trends in wind speed at the LLJ core, and also at the fixed level of 100 m (not shown). Close to the surface (2–10 m), previously reported trends in wind speed are negative in different parts of the world (McVicar et al., 2012). The authors point to a global decrease in the wind speed near the surface, based

on the results from different studies. The results discussed here concern the past changes of LLJs. Future trends may not necessarily be the same. For example, Semedo et al. (2016) assessed changes in CLLJs, through experiments with the CMIP5 model EC-Earth for future scenarios. The model projected the largest regional increase in the frequency of occurrence, intensity, and height of LLJs for the Iberian Peninsula and the Oman CLLJs. CLLJ regions show in their study negative trends in the LLJ core wind speed, for example, in Western USA and West Africa. Based on regional climate model output, Torres-Alavez et al. (2021) point to a future increase of the LLJ intensity and spatial coverage in different regions, for example, in West Africa and the Caribbean. Similar to the future development seen by the latter study, we detected an increase in the frequency of the occurrence of LLJ profiles in the Caribbean and LLJ intensity in West Africa in the past decades. However, differences were also found as one would expect for comparing different time periods and data sets.

LLJs also have impacts on wind power production, for example, offshore wind power due to the high frequency of occurrence of CLLJs. Locations with more frequent and more intense CLLJs can be strongly affected since wind speed at the rotor layer can be strongly connected to the LLJ intensities. However, negative impacts on the wind turbines shall be also taken into consideration due to the higher shear connected to LLJs (E. W. Luiz & Fiedler, 2022). In addition, long LLJ events can also decrease the wind variability (Kamath, 2010; Wimhurst & Greene, 2019), having a positive impact on the stability of electricity production. An increased duration of LLJs could therefore reduce the occurrence of ramp events, that is, sharp gradients in the amount of generated electricity, in offshore areas (CLLJs) as well as over land (NLLJs).

5. Conclusion

A global climatology of low-level jets (LLJs) based on ERA5 was compiled with a focus on different driving mechanisms. The analysis encompasses the years 1992–2021 using the latest ECMWF reanalysis. Given the improvements in ERA5 compared to its predecessors for LLJ analysis (Lima et al., 2022), particularly the higher spatial and temporal resolution, improved data assimilation schemes, and an increased amount of assimilated observations, this study was able to analyze regional circulation features and characteristics of the associated LLJs.

The global mean frequency of occurrence was 21%, with averages of 32% and 15% over land and ocean. The results were also presented over three specific regions with some differences in the main LLJ formation mechanism, as follows: non-polar land (LLLJ), polar (PLLJ), and coastal LLJs (CLLJ). The results highlight the following findings:

- Over LLLJ areas, the most common LLJ type follows the NLLJ formation mechanism, which is based on the classical theory of inertial oscillation over land. Interestingly, NLLJs are not dominating the LLJ formation from a global perspective, with mean occurrence frequencies of 20% over LLLJ regions with some exceptions. For instance, the Bodélé Depression stands out as an important desert NLLJ hotspot from the global perspective.
- Over PLLJ areas, NLLJ can also occur very frequently, especially due to the prolonged stable and shallow boundary layer in polar winter, making the PLLJs the lowest and strongest LLJ amongst the categories assessed. However, due to their extremely high frequencies with values partly exceeding 90% also during polar days, they can be further favored by other factors than nocturnal cooling, for example, due to the cold surfaces and katabatic winds over the ice shelf (Heinemann et al., 2021; Jakobson et al., 2013).
- CLLJs have different characteristics compared to NLLJs and PLLJs. There is no surface temperature inversion co-occurring with CLLJs but an elevated inversion layer around the core of the CLLJ that maintains their stability. Despite a similar frequency of occurrence to LLLJ regions (19%), CLLJs occur around 90% of the time in hotspots often situated on the west coast of continents. The favorable conditions for the CLLJ formation may arise due to the subsidence of air in the trades and the advection of hot desert air over the relatively cool marine boundary layer over regions affected by coastal upwelling.

Our trend analysis indicates past changes in both the frequency and intensity of regional LLJs, including areas with major sources of dust aerosols, polar ice, and atmospheric moisture. The here-released data for LLJs can be used for more detailed assessments of the regional LLJs and their role in other processes in future studies. Moreover, the implications of the past changes of LLJs documented here and potential future trends of LLJs as seen in other studies (Torres-Alavez et al., 2021) in the Earth system are unclear, which future studies can address to better understand the role of LLJs in a warming world.

Data Availability Statement

The ERA5 data set is available on the Copernicus Climate Change Service Information website (<https://cds.climate.copernicus.eu>, last access 20 March 2024). The Radiosondes data can be obtained from the department of Atmospheric Science of the University of Wyoming (<https://weather.uwyo.edu/upperair/sounding.html>, last access 20 March 2024).

The generated data for the ERA5-based LLJs occurrence and characteristics are available via E. W. Luiz et al. (2023).

Acknowledgments

We thank the anonymous reviewer and the editor for the appraisal of our manuscript. The financial support for this research encompasses contributions from the Max-Planck-Institute for Meteorology for hiring a student assistant and the Hans-Ertel-Centre for Weather Research (HErZ “Climate Monitoring and Diagnostic” phase III, Grant BMVI/DWD 4818DWDPA) for hiring Eduardo Weide Luiz. This work used resources of the Deutsches Klimarechenzentrum (DKRZ) Granted by its Scientific Steering Committee (WLA) under project ID bb1198.

References

- Algarra, I., Eiras-Barca, J., Nieto, R., & Gimeno, L. (2019). Global climatology of nocturnal low-level jets and associated moisture sources and sinks. *Atmospheric Research*, 229, 39–59. <https://doi.org/10.1016/j.atmosres.2019.06.016>
- Amador, J. A., Alfaro, E. J., Rivera, E. R., & Calderón, B. (2010). Climatic features and their relationship with tropical cyclones over the intra-Americas seas. *Hurricanes and Climate Change*, 2, 149–173. https://doi.org/10.1007/978-90-481-9510-7_9
- Amador Astúa, J. A. (1998). A climate feature of the tropical Americas: The trade wind easterly jet.
- Angevine, W. M., Tjernström, M., & Žagar, M. (2006). Modeling of the coastal boundary layer and pollutant transport in New England. *Journal of Applied Meteorology and Climatology*, 45(1), 137–154. <https://doi.org/10.1175/jam2333.1>
- Arrau, J. M., Nobre, C., Barbosa, H. M., Obregon, G., & Marengo, J. (2012). Aerial rivers and lakes: Looking at large-scale moisture transport and its relation to Amazonia and to subtropical rainfall in South America. *Journal of Climate*, 25(2), 543–556. <https://doi.org/10.1175/2011jcli4189.1>
- Beardsley, R., Dorman, C., Friehe, C., Rosenfeld, L., & Winant, C. (1987). Local atmospheric forcing during the coastal ocean dynamics experiment: I. A description of the marine boundary layer and atmospheric conditions over a northern California upwelling region. *Journal of Geophysical Research*, 92(C2), 1467–1488. <https://doi.org/10.1029/jc092ic02p01467>
- Beyrich, F. (1994). Sodar observations of the stable boundary layer height in relation to the nocturnal low-level jet. *Meteorologische Zeitschrift. Neue Folge (Berlin)*, 3(1), 29–34. <https://doi.org/10.1127/metz/3/1/1994/29>
- Blackadar, A. K. (1957). Boundary layer wind maxima and their significance for the growth of nocturnal inversions. *Bulletin of the American Meteorological Society*, 38(5), 283–290. <https://doi.org/10.1175/1520-0477-38.5.283>
- Chen, G. T.-J., Wang, C.-C., & Lin, L.-F. (2006). A diagnostic study of a retreating Mei-Yu front and the accompanying low-level jet formation and intensification. *Monthly Weather Review*, 134(3), 874–896. <https://doi.org/10.1175/mwr3099.1>
- Chen, R., & Tomassini, L. (2015). The role of moisture in summertime low-level jet formation and associated rainfall over the East Asian monsoon region. *Journal of the Atmospheric Sciences*, 72(10), 3871–3890. <https://doi.org/10.1175/jas-d-15-0064.1>
- Corrêa, P. B., Dias-Júnior, C. Q., Cava, D., Sörgel, M., Botía, S., Acevedo, O., et al. (2021). A case study of a gravity wave induced by amazon forest orography and low level jet generation. *Agricultural and Forest Meteorology*, 307, 108457. <https://doi.org/10.1016/j.agrformet.2021.108457>
- Fiedler, S., Schepanski, K., Heinold, B., Knippertz, P., & Tegen, I. (2013). Climatology of nocturnal low-level jets over North Africa and implications for modeling mineral dust emission. *Journal of Geophysical Research: Atmospheres*, 118(12), 6100–6121. <https://doi.org/10.1002/jgrd.50394>
- Garreaud, R., & Muñoz, R. C. (2005). The low-level jet off the west coast of subtropical South America: Structure and variability. *Monthly Weather Review*, 133(8), 2246–2261. <https://doi.org/10.1175/mwr2972.1>
- Gimeno, L., Dominguez, F., Nieto, R., Trigo, R., Drumond, A., Reason, C. J., et al. (2016). Major mechanisms of atmospheric moisture transport and their role in extreme precipitation events. *Annual Review of Environment and Resources*, 41(1), 117–141. <https://doi.org/10.1146/annurev-environ-110615-085558>
- Gutiérrez, W., Araya, G., Kiliyanpilakkil, P., Ruiz-Columbie, A., Tutkun, M., & Castillo, L. (2016). Structural impact assessment of low level jets over wind turbines. *Journal of Renewable and Sustainable Energy*, 8(2), 023308. <https://doi.org/10.1063/1.4945359>
- Han, Y., Yang, Q., Liu, N., Zhang, K., Qing, C., Li, X., et al. (2021). Analysis of wind-speed profiles and optical turbulence above Gaomeigu and the Tibetan Plateau using ERA5 data. *Monthly Notices of the Royal Astronomical Society*, 501(4), 4692–4702. <https://doi.org/10.1093/mnras/staa2960>
- Han, Z., Ge, J., Chen, X., Hu, X., Yang, X., & Du, J. (2022). Dust activities induced by nocturnal low-level jet over the Taklimakan desert from WRF-Chem simulation. *Journal of Geophysical Research: Atmospheres*, 127(12), e2021JD036114. <https://doi.org/10.1029/2021jd036114>
- Heinemann, G., Drüe, C., Schwarz, P., & Makshtas, A. (2021). Observations of wintertime low-level jets in the coastal region of the Laptev Sea in the Siberian Arctic using SODAR/RASS. *Remote Sensing*, 13(8), 1421. <https://doi.org/10.3390/rs13081421>
- Heinemann, G., & Zentek, R. (2021). A model-based climatology of low-level jets in the Weddell Sea region of the Antarctic. *Atmosphere*, 12(12), 1635. <https://doi.org/10.3390/atmos12121635>
- Heinold, B., Knippertz, P., Marsham, J., Fiedler, S., Dixon, N., Schepanski, K., et al. (2013). The role of deep convection and nocturnal low-level jets for dust emission in summertime West Africa: Estimates from convection-permitting simulations. *Journal of Geophysical Research: Atmospheres*, 118(10), 4385–4400. <https://doi.org/10.1002/jgrd.50402>
- Hersbach, H., Bell, B., Berrisford, P., Hirahara, S., Horányi, A., Muñoz-Sabater, J., et al. (2020). The ERA5 global reanalysis. *Quarterly Journal of the Royal Meteorological Society*, 146(730), 1999–2049. <https://doi.org/10.1002/qj.3803>
- Jakobson, L., Vihma, T., Jakobson, E., Palo, T., Männik, A., & Jaagus, J. (2013). Low-level jet characteristics over the Arctic ocean in spring and summer. *Atmospheric Chemistry and Physics*, 13(21), 11089–11099. <https://doi.org/10.5194/acp-13-11089-2013>
- Kamath, C. (2010). Understanding wind ramp events through analysis of historical data. In *IEEE PES T&D 2010* (pp. 1–6).
- Knippertz, P., & Todd, M. C. (2012). Mineral dust aerosols over the Sahara: Meteorological controls on emission and transport and implications for modeling. *Reviews of Geophysics*, 50(1), RG1007. <https://doi.org/10.1029/2011rg000362>
- Lampert, A., Bernalte Jimenez, B., Gross, G., Wulff, D., & Kenull, T. (2016). One-year observations of the wind distribution and low-level jet occurrence at Braunschweig, North German Plain. *Wind Energy*, 19(10), 1807–1817. <https://doi.org/10.1002/we.1951>
- Li, X., & Du, Y. (2021). Statistical relationships between two types of heavy rainfall and low-level jets in South China. *Journal of Climate*, 34(21), 8549–8566. <https://doi.org/10.1175/jcli-d-21-0121.1>

- Lima, D. C., Soares, P. M., Nogueira, M., & Semedo, A. (2022). Global coastal low-level wind jets revisited through the new ERA5 reanalysis. *International Journal of Climatology*, *42*(9), 4491–4507. <https://doi.org/10.1002/joc.7482>
- Lima, D. C., Soares, P. M., Semedo, A., Cardoso, R. M., Cabos, W., & Sein, D. V. (2019). A climatological analysis of the Benguela coastal low-level jet. *Journal of Geophysical Research: Atmospheres*, *124*(7), 3960–3978. <https://doi.org/10.1029/2018jd028944>
- Luiz, E., & Fiedler, S. (2023). Can convective cold pools lead to the development of low-level jets? *Geophysical Research Letters*, *50*(11), e2023GL103252. <https://doi.org/10.1029/2023gl103252>
- Luiz, E. W., & Fiedler, S. (2022). Spatiotemporal observations of nocturnal low-level jets and impacts on wind power production. *Wind Energy Science*, *7*(4), 1575–1591. <https://doi.org/10.5194/wes-7-1575-2022>
- Luiz, E. W., Fiedler, S., & Wahl, S. (2023). ERA5 global climatology of low-level jets. *DOKU at DKRZ*. Retrieved from https://www.wdc-climate.de/ui/entry?acronym=DKRZ_LTA_1198_ds00001
- Luna-Niño, R., & Cavazos, T. (2018). Formation of a coastal barrier jet in the Gulf of Mexico due to the interaction of cold fronts with the Sierra Madre Oriental mountain range. *Quarterly Journal of the Royal Meteorological Society*, *144*(710), 115–128. <https://doi.org/10.1002/qj.3188>
- McVicar, T. R., Roderick, M. L., Donohue, R. J., Li, L. T., Van Niel, T. G., Thomas, A., et al. (2012). Global review and synthesis of trends in observed terrestrial near-surface wind speeds: Implications for evaporation. *Journal of Hydrology*, *416*, 182–205. <https://doi.org/10.1016/j.jhydrol.2011.10.024>
- Pan, Z., Segal, M., & Arritt, R. W. (2004). Role of topography in forcing low-level jets in the central United States during the 1993 flood-altered terrain simulations. *Monthly Weather Review*, *132*(1), 396–403. [https://doi.org/10.1175/1520-0493\(2004\)132<0396:rotifl>2.0.co;2](https://doi.org/10.1175/1520-0493(2004)132<0396:rotifl>2.0.co;2)
- Peng, Y., Yu, Q., Du, Z., Wang, L., Wang, Y., & Gao, S. (2022). The dynamics of wave and current supported gravity flows: Evaluation of drag coefficient and bulk Richardson number. *Marine Geology*, *454*, 106947. <https://doi.org/10.1016/j.margeo.2022.106947>
- Prospero, J. M., Ginoux, P., Torres, O., Nicholson, S. E., & Gill, T. E. (2002). Environmental characterization of global sources of atmospheric soil dust identified with the nimbus 7 total ozone mapping spectrometer (toms) absorbing aerosol product. *Reviews of Geophysics*, *40*(1), 2-1–2-31. <https://doi.org/10.1029/2000rg000095>
- Ranjha, R., Svensson, G., Tjernström, M., & Semedo, A. (2013). Global distribution and seasonal variability of coastal low-level jets derived from ERA-interim reanalysis. *Tellus A: Dynamic Meteorology and Oceanography*, *65*(1), 20412. <https://doi.org/10.3402/tellusa.v65i0.20412>
- Ranjha, R., Tjernström, M., Semedo, A., Svensson, G., & Cardoso, R. M. (2015). Structure and variability of the Oman coastal low-level jet. *Tellus A: Dynamic Meteorology and Oceanography*, *67*(1), 25285. <https://doi.org/10.3402/tellusa.v67.25285>
- Schepanski, K., Tegen, I., Todd, M. C., Heinold, B., Bönišch, G., Laurent, B., & Macke, A. (2009). Meteorological processes forcing Saharan dust emission inferred from MSG-SEVIRI observations of subdaily dust source activation and numerical models. *Journal of Geophysical Research*, *114*(D10), D10201. <https://doi.org/10.1029/2008JD010325>
- Semedo, A., Soares, P. M., Lima, D. C., Cardoso, R. M., Bernardino, M., & Miranda, P. M. (2016). The impact of climate change on the global coastal low-level wind jets: EC-EARTH simulations. *Global and Planetary Change*, *137*, 88–106. <https://doi.org/10.1016/j.gloplacha.2015.12.012>
- Shapiro, A., & Fedorovich, E. (2010). Analytical description of a nocturnal low-level jet. *Quarterly Journal of the Royal Meteorological Society*, *136*(650), 1255–1262. <https://doi.org/10.1002/qj.628>
- Sisterson, D. L., & Frenzen, P. (1978). Nocturnal boundary-layer wind maxima and the problem of wind power assessment. *Environmental Science & Technology*, *12*(2), 218–221. <https://doi.org/10.1021/es60138a014>
- Soares, P. M., Cardoso, R. M., Semedo, A., Chinita, M. J., & Ranjha, R. (2014). Climatology of the Iberia coastal low-level wind jet: Weather research forecasting model high-resolution results. *Tellus A: Dynamic Meteorology and Oceanography*, *66*(1), 22377. <https://doi.org/10.3402/tellusa.v66.22377>
- Torres-Alavez, J. A., Das, S., Corrales-Suastegui, A., Coppola, E., Giorgi, F., Raffaele, F., et al. (2021). Future projections in the climatology of global low-level jets from CORDEX-CORE simulations. *Climate Dynamics*, *57*(5–6), 1–19. <https://doi.org/10.1007/s00382-021-05671-6>
- Tuononen, M., Sinclair, V., & Vihma, T. (2015). A climatology of low-level jets in the mid-latitudes and polar regions of the Northern Hemisphere. *Atmospheric Science Letters*, *16*(4), 492–499. <https://doi.org/10.1002/asl.587>
- Van de Wiel, B., Moene, A., Hartogensis, O., De Bruin, H., & Holtslag, A. (2003). Intermittent turbulence in the stable boundary layer over land. Part III: A classification for observations during cases-99. *Journal of the Atmospheric Sciences*, *60*(20), 2509–2522. [https://doi.org/10.1175/1520-0469\(2003\)060<2509:ititsb>2.0.co;2](https://doi.org/10.1175/1520-0469(2003)060<2509:ititsb>2.0.co;2)
- Van de Wiel, B. J. H., Moene, A. F., Steeneveld, G. J., Baas, P., Bosveld, F. C., & Holtslag, A. A. M. (2010). A conceptual view on inertial oscillations and nocturnal low-level jets. *Journal of the Atmospheric Sciences*, *67*(8), 2679–2689. <https://doi.org/10.1175/2010JAS3289.1>
- Washington, R., Todd, M., Middleton, N. J., & Goudie, A. S. (2003). Dust-storm source areas determined by the total ozone monitoring spectrometer and surface observations. *Annals of the Association of American Geographers*, *93*(2), 297–313. <https://doi.org/10.1111/1467-8306.9302003>
- Wimhurst, J. J., & Greene, J. S. (2019). Oklahoma's future wind energy resources and their relationship with the central plains low-level jet. *Renewable and Sustainable Energy Reviews*, *115*, 109374. <https://doi.org/10.1016/j.rser.2019.109374>
- Wittich, K. P., Hartmann, J., & Roth, R. (1986). On nocturnal wind shear with a view to engineering applications. *Boundary-Layer Meteorology*, *37*(3), 215–227. <https://doi.org/10.1007/bf00122985>
- Zemp, D., Schleussner, C.-F., Barbosa, H., Van der Ent, R., Donges, J. F., Heinke, J., et al. (2014). On the importance of cascading moisture recycling in South America. *Atmospheric Chemistry and Physics*, *14*(23), 13337–13359. <https://doi.org/10.5194/acp-14-13337-2014>
- Ziemann, A., Galvez Arboleda, A., & Lampert, A. (2020). Comparison of wind lidar data and numerical simulations of the low-level jet at a grassland site. *Energies*, *13*(23), 6264. <https://doi.org/10.3390/en13236264>